

Glowworm Swarm Optimization for Photovoltaic Model Identification

Hugo Nunes, José Pombo, João Fermeiro, Sílvio Mariano, Maria do Rosário Calado
University of Beira Interior and Instituto de Telecomunicações

Covilhã, Portugal

Emails: hugo.garcia.nunes@hotmail.com; jose_p@portugalmail.com; fermeiro@ubi.pt; sm@ubi.pt; rc@ubi.pt

Abstract—This paper presents a new algorithm for finding the parameters that characterize a photovoltaic panel by using the Glowworm Swarm Optimization algorithm. This new algorithm shows great simplicity, flexibility and precision, being able to precisely locate the global optimum point or multiple global optimum points, independently of the initial conditions. The approach here adopted allows the utilization of the algorithm in several existing models to characterize a photovoltaic panel in the current literature.

Index Terms—Glowworm Swarm Optimization, Photovoltaic module, Modelling, Simulation.

I. INTRODUCTION

The development of reliable modelling techniques of photovoltaic (PV) modules is of primary concern because it allows the designer to optimize the performance and the cost effectiveness of the system. The aim of this paper is to characterize accurately photovoltaic systems, introducing new models to obtain the photovoltaic panel parameters' when operating under different conditions, chiefly the temperature and radiation.

There are several approaches that can be found in the literature, being the most recurrent one the resolution of a system of nonlinear equations. Numerical methods are required in order to determine the parameters that characterize the model under the reference conditions, by employing three to five fundamental working points of the characteristic curve. The mentioned working points are the maximum power point; the short-circuit point; the open circuit point; and also two more intermediate points, referred by other authors, such as the current corresponding to the average point between V_{oc} and V_{mpp} (called I_{xx}) and the current corresponding to the average point between 0 and V_{mpp} (called I_x) [1]–[5].

Iterative methods to estimate mathematical model parameters that characterize the photovoltaic panel are, however, used to avoid the considerable computational effort necessary to solve the system of nonlinear equations [6]–[8]. In addition, by using the Lambert W function, the mathematical model can be expressed as an explicit formula, which consists in another solution proposed in the literature [9], [10]. Yet, there are other authors who choose alternative methodologies that involve the utilization of artificial intelligent techniques, for example Neural Networks [11], [12] and Fuzzy Logic [13]. Although Neural Networks and Fuzzy Logic can be powerful tools, for highly dynamic systems in adaptive computation

with parallel processing and competent information to deal with the nonlinear characteristics of the photovoltaic panels, they need large computational time and/or training.

Another methodology involving Artificial Intelligence techniques suited to deal with nonlinear characteristics is the Swarm Intelligence [14]–[16]. However, this algorithm only allows to locate with precision the global optimum point.

Therefore, by using the Glowworm Swarm Optimization, several fundamental aspects are pointed out throughout this paper: (i) the algorithm is capable to locate with precision both the global optimum point and the multiple global optimum, independently of the initial conditions; (ii) it only makes use of the information provided by the manufacturer datasheet, avoiding the need to carry out experimental data; (iii) it is a simple and extremely flexible method, which presents a reasonable convergence time (depending of the stopping criterion, obviously); (iv) it can be applied to any existing mathematical model; and, finally, (v) it can be used out of the standard conditions (STC), employing for that an extrapolation method, namely the Blaesser method [17], the Anderson method [18] and the Marion method [19]. Each method is valid in some radiation and temperature intervals.

This paper is organized in five sections. In the second one is presented a bibliographical revision of the main models that characterize a photovoltaic panel; in section 3, a description as well as a general conception of the Glowworm Swarm Optimization algorithm is done; in section 4, the one-diode mathematical model parameters obtained by using the new technique and the proposed algorithm are presented. Finally, the last section concludes the paper.

II. MATHEMATICAL MODELS

Several models are proposed in the literature with the aim of simulating the photovoltaic cells operating behavior under different conditions. The main models that represent the photovoltaic cell are: the one-diode model [20], [21], the two-diodes model [22]–[24] and the multi-diodes model [25]. The one-diode model, Fig.(1), is characterized by five parameters: the photoelectric current I_{ph} , proportional to the irradiance, the reverse saturation current of the diode I_{sat} , its ideality factor m , the resistor R_s , and the resistor R_p . Approximated models can be derived from Eq.(1) considering the R_p resistor infinite (four parameters model) or the diode ideality factor as ideal allied to the previous condition (three parameters model).

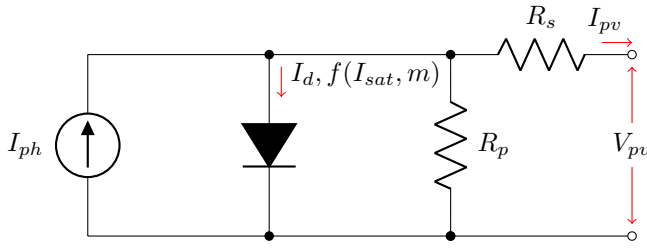


Figure 1. One-diode mathematical model of a photovoltaic cell.

Applying Kirchhoff's laws to the circuit of Fig.(1) the equation that describes the circuit current is given by Eq.(1),

$$I = I_{ph} - I_d - \frac{V + I \times R_s}{R_p} \quad (1)$$

in which,

$$I_d = I_{sat} \left[\exp \left(\frac{(V + I \times R_s)}{mV_t} \right) - 1 \right] \quad (2)$$

and

$$V_t = \frac{kT}{q} \quad (3)$$

where, V_t is the thermal voltage of the photovoltaic cell, q is the electron charge ($1.60217646 \times 10^{-19}$ C), k is the Boltzmann constant ($1.3806503 \times 10^{-23}$ J/K) and T is the temperature of the p-n junction in Kelvin.

III. GLOWWORM SWARM OPTIMIZATION

The Glowworm Swarm Optimization algorithm [26]–[28] is inspired by the behavior of the Coleoptera insects (firefly or glowworm) that produce a bioluminescence substance which is called luciferin and is used to attract the female. The males are as more attractive as they produce a higher amount of luciferin.

The idea behind the algorithm is to evolve the agents (fireflies) with lesser attributes of luciferin towards the agents with a higher level of luciferin. Nevertheless, each agent is endowed with a behavior mechanism that allows them to selectively interact with its neighbors and decide its progress in each iteration.

In the algorithm this level of luciferin is calculated through the Eq.(4), where ℓ_t, ℓ_{t-1} are the luciferin values at the instant t and at the instant $t-1$, respectively, ρ is the rate of decay of luciferin whose value lays in the interval $0 \leq \rho \leq 1$, and δ is a weight factor for the value of the function of agent i at the instant t .

$$\ell_t = (1 - \rho)\ell_{t-1} + \delta F(x_i(t)) \quad (4)$$

As it has been said previously, each agent is endowed with a behavior mechanism that affects its field of perception which is enclosed in a circle of radius r_{t+1}^i given by Eq.(5) which is adjusted in each iteration.

$$r_{t+1}^i = \min \{ r_{\max}, \max \{ 0, r_t^i + \beta(n_t - N_i(t)) \} \} \quad (5)$$

in which

$$N_i(t) = \{ j : d_{ij} < r_t^i; \ell_i < \ell_j \} \quad (6)$$

The neighborhood of the agent i is formed by the agents j whose distances are smaller than r_t^i and its attribute of luciferin is greater than the amount of luciferin of agent i . Eq.(6) represents the number of neighbors at the instant t , where d_{ij} is the Euclidian distance between the two agents i and j .

With the aim to control the number of neighbors, two constants are introduced in Eq.(5), namely n_t and r_{\max} . These two parameters allow movements based in local information (i.e., with a small radius of perception), separating the agents in subgroups that converge to multiple local maximums of the fitness function, or, instead, allowing movements based in global information (i.e., with a large radius of perception), that lead the agents to converge to a global optimum of the fitness function.

In the so called classic algorithm, if an agent does not have another agent within its radius of perception, then it will remain in its position until another agent, with better attribute of luciferin, comes inside its radius of perception. However, in the algorithm implemented this does not happens, it will move in a random way as function of another agent. The movement of each agent is a function of its field of perception and also of the probability function described by Eq.(7), where $p_{ij}(t)$ is the probability of the agent i to choose the agent j belonging to its field of perception.

$$p_{ij}(t) = \frac{\ell_j(t) - \ell_i(t)}{\sum_{k \in N_i(t)} \ell_k(t) - \ell_i(t)} \quad (7)$$

After a selection based on the function of Eq.(7) the agents should update their new position through Eq.(8), where s is a weight factor for the amplitude of the step that the agent i will give.

$$x_i(t+1) = x_i(t) + s \left(\frac{x_j(t) - x_i(t)}{\|x_j(t) - x_i(t)\|} \right) \quad (8)$$

For this type of problem, the Glowworm Swarm Optimization is implemented accordingly to Alg.(1).

Algorithm 1 Glowworm Swarm Optimization Algorithm

```

1: Define the dimension of the problem;
2: Define the number of agents  $\rightarrow n$ ;
3: Define the step  $\rightarrow s$ ;
4: Positioning the agents in the search region;
5: for  $i = 1 : n$  do
6:    $\ell_i = \ell_0$ 
7:    $r_i^n = r_0$ 
8: end for
9: Define the maximum number of iterations  $\rightarrow iter_{max}$ ;
10: while  $iter < iter_{max}$  do
11:   for  $i = 1 : n$  do
12:      $\ell_{i,(iter)} = (1 - \rho) \ell_{i,(iter-1)} + \delta F(x_{i,iter})$ 
13:   end for
14:   for  $i = 1 : n$  do
15:      $N_i(t) = \{j : d_{ij} < r_i^i; \ell_i < \ell_j\}$ 
16:     for  $i = 1 : j \in N_i(t)$  do
17:        $p_{ij}(t) = \frac{\ell_j(t) - \ell_i(t)}{\sum_{k \in N_i(t)} \ell_k(t) - \ell_i(t)}$ 
18:     end for
19:     Select the agent  $j$  by the probability function;
20:      $x_i(t+1) = x_i(t) + s \left( \frac{x_j(t) - x_i(t)}{\|x_j(t) - x_i(t)\|} \right)$ 
21:      $r_{t+1}^i = \min \{r_{max}, \max \{0, r_t^i + \beta (n_t - N_i(t))\}\}$ 
22:   end for
23: end while

```

With the aim of testing and simulate the procedure previously described, the algorithm was implemented in a simulation environment using the software Matlab. The objective function is expressed by the Eq.(9) and the parameters used are shown in Tab.(I).

$$f(x, y) = 3(1-x)^2 \exp(-x^2 - (y+1)^2) - 10 \left(\frac{x}{5} - x^3 - y^5 \right) \exp(-x^2 - y^2) - \frac{1}{3} \exp(-(x+1)^2 - y^2) \quad (9)$$

Table I
GLOWWORM SWARM OPTIMIZATION PARAMETERS

Parameters	n_t	r_{max}	s	γ	β	ρ
Experiment 1	30	0.1	0.01	0.6	0.08	0.4
Experiment 2	200	10	0.01	0.6	0.08	0.4

In the experiments held, two hundred agents have been used, and they were initially located in the search region on a linear form. In experiment 1, only movements based on local information were allowed. This kind of behavior mechanism is implemented using two parameters, n_t and r_{max} , that affect the perception radius of each agent in each iteration. Fig.(2) illustrate the performance of the algorithm, where it can be seen that all the maximum points of the function were reached once the maximum allowed radius of perception of the agents is small. However, in experiment 2 it was increased the maximum radius (up to the limit, which was the whole

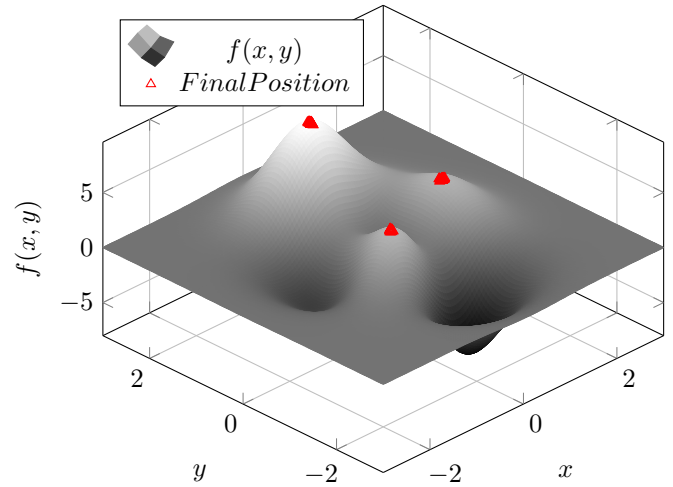


Figure 2. Behavior of Glowworm Swarm algorithm with local information.

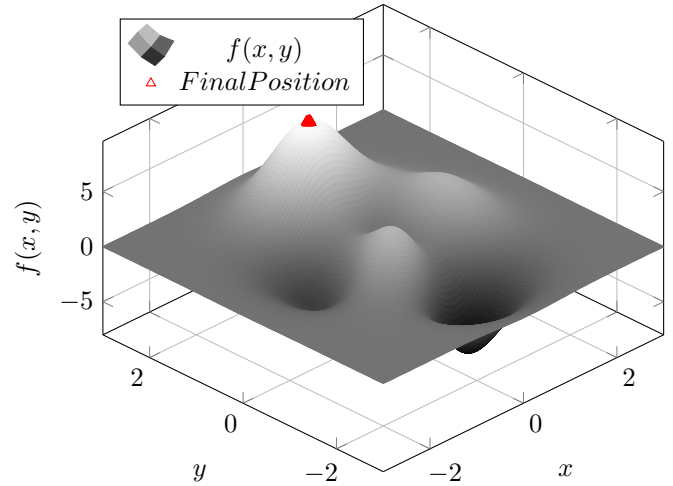


Figure 3. Behavior of Glowworm Swarm algorithm with global information.

search region) and it was allowed that the desired number of neighbors should be the population. Then, the movements of all agents have converged to the global maximum as it can be seen in Fig.(3).

IV. EXPERIMENTAL RESULTS

Once implemented and tested, the algorithm was applied to the case under consideration here in order to determine the parameters that characterize the one-diode model (which corresponds to Eq.(1)), as well as their optimum values of these parameters. This model guarantees the compromise between simplicity and precision and is used by several authors. The fact that Eq.(1) does not admit an explicit solution reveals a significant limitation, not only for the parameter identification of the model, as already mentioned before, but also in the simulation. This limitation can be overcome through the Lambert W function used by several authors [4], [9], [10]. By using Lambert W function one gets expression (10) and (11).

Table II
PARAMETERS OF THE PHOTOVOLTAIC PANEL SHARP ND-R250A5.

N_S	60	V_{mpp}	30.9 V
I_{mpp}	8.10 A	α_v	-0.329 (%/C)
V_{OC}	37.6 V	α_i	0.038 (%/C)
I_{SC}	8.68 A	P_{mpp}	250 W

$$I = \frac{R_p (I_{ph} + I_{sat}) - V}{R_s + R_p} - \frac{mV_t}{R_s} \text{lambertW}(\theta) \quad (10)$$

in which θ is given by the Eq.(11)

$$\theta = \frac{\left(\frac{R_p R_s}{R_p + R_s}\right) I_{sat} \exp\left(\frac{R_p R_s (I_{ph} + I_{sat}) + R_p V}{mV_t (R_p + R_s)}\right)}{mV_t} \quad (11)$$

Observing Eqs.(10) and (11), the expressions are now explicit, so that, for any voltage value the corresponding value of current can be calculated directly. Another solution that is found in the literature to overcome this constraint is the use of numerical methods, such as the Newton-Raphson.

In the proposed Glowworm Swarm optimization algorithm, it was employed the photovoltaic panel Sharp ND-R250A5, whose parameters have been summarized in Tab.(II). The optimization algorithm consists on the variation of the values of the resistors R_s , R_p and the ideality factor m that characterize the model of Fig.(1) which corresponds to Eq.(1), maximizing the multi-objective function given by the expressions in Eqs.(12) and (13):

$$f(R_s, R_p, m) = \max\left(\frac{1}{F}\right) \quad (12)$$

$$F = \left| \begin{array}{l} P_{mpp \rightarrow STC} - P_{mpp \rightarrow (m, R_s, R_p)} \\ V_{mpp \rightarrow STC} - V_{mpp \rightarrow (m, R_s, R_p)} \\ I_{mpp \rightarrow STC} - I_{mpp \rightarrow (m, R_s, R_p)} \end{array} \right| + \quad (13)$$

In the proposed optimization algorithm movements based on local information were allowed, letting the agents to converge to the multiple global optimum points. The multi-objective function consists on the determination of the working point that corresponds to the maximum power, but it is necessary to guarantee that this point occurs in the corresponding value of pair voltage-current, indicated on the manufacturer data-sheet, otherwise the working point that corresponds to the maximum power can be reached by a different voltage-current pair. The algorithm for determining the R_s , R_p resistors and the ideality factor m is implemented accordingly to Alg.(2).

The Fig.(4) illustrates the variation of the resistor R_s as function of the diode ideality factor m and Fig.(5) illustrate the variation of the resistor R_s as function of the resistor R_p . Analyzing the figures, we can conclude that: (i) the photovoltaic parameter extraction is a very hard multimodal problem, since the algorithm converged to several local minima; (ii) for values of the resistor R_s over 0.5, independently of the remaining parameters, the solution does not lie close to the theoretical

Algorithm 2 Algorithm for determining the R_s and R_p resistors and the ideality factor m .

- 1: Define the dimension of the problem;
- 2: Define the number of agents $\rightarrow n$;
- 3: Define the step $\rightarrow s$;
- 4: Positioning the agents in the search region;
- 5: Define the number of points to discretize $V \in 0 \leq V \leq V_{oc} \rightarrow n_v$;
- 6: **for** $i = 1 : n$ **do**
- 7: $\ell_i = \ell_0$
- 8: $r_i^n = r_0$
- 9: **end for**
- 10: Define the maximum number of iterations $\rightarrow iter_{max}$;
- 11: **while** $iter < iter_{max}$ **do**
- 12: **for** $i = 1 : n$ **do**
- 13: Calculate the dependent parameters of the m factor;
- 14: **for** $j = 1 : n_v$ **do**
- 15: $\theta(j) = \frac{\left(\frac{R_p(i)R_s(i)}{R_p(i)+R_s(i)}\right) I_{sat}(y) x \exp\left(\frac{R_p(i)R_s(i)(I_{ph}+I_{sat}(i))+R_p(i)V(j)}{m(i)V_t(R_p(i)+R_s(i))}\right)}{m(i)V_t}$
- 16: $I(j) = \frac{R_p(i)(I_{ph}+I_{sat}(i))-V(j)}{R_s(i)+R_p(i)} - \frac{m(i)V_t}{R_s(i)} \text{lambertW}(\theta(j))$
- 17: **end for**
- 18: Find the maximum value of $V(j)I(j)$;
- 19: Evaluate F;
- 20: $\ell_{i,(iter)} = (1 - \rho) \ell_{i,(iter-1)} + \delta F(x_{i,iter})$
- 21: **end for**
- 22: **for** $i = 1 : n$ **do**
- 23: $N_i(t) = \{j : d_{ij} < r_i^i, \ell_i < \ell_j\}$
- 24: **for** $i = 1 : j \in N_i(t)$ **do**
- 25: $p_{ij}(t) = \frac{\ell_j(t) - \ell_i(t)}{\sum_{k \in N_i(t)} \ell_k(t) - \ell_i(t)}$
- 26: **end for**
- 27: Select the agent j by the probability function;
- 28: $x_i(t+1) = x_i(t) + s \left(\frac{x_j(t) - x_i(t)}{\|x_j(t) - x_i(t)\|}\right)$
- 29: $r_{i,t+1} = \min\{r_{max}, \max\{0, r_i^i + \beta(n_t - N_i(t))\}\}$
- 30: **end for**
- 31: **end while**

solution, which is 250 W; (iii) for the diode ideality factor m values over 1.2, independently of the remaining parameters, the solution does not lie close to the theoretical solution; (iv) by increasing the values of the ideality factor m , the solutions become close to the theoretical solution, requiring a reduction of the value of the resistors R_s ; (v) resistor R_p can reach an infinite value.

The Fig.(6) and Fig.(7) illustrates the characteristics curves of the pair voltage-current and voltage-power of the ten best solutions found, whose parameters are summarized in the Tab.(III). The proposed method holds great flexibility, simplicity and precision, being used for any existing model, performing both under the reference conditions as well as out off these conditions. This study allowed to conclude that: (i) the assumption that resistor R_p is infinite, by the point

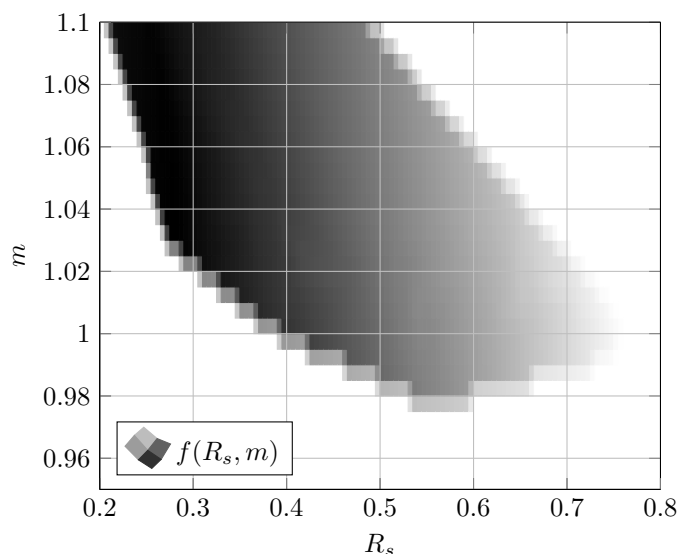


Figure 4. Variation of the resistor R_s as function of the diode ideality factor m .

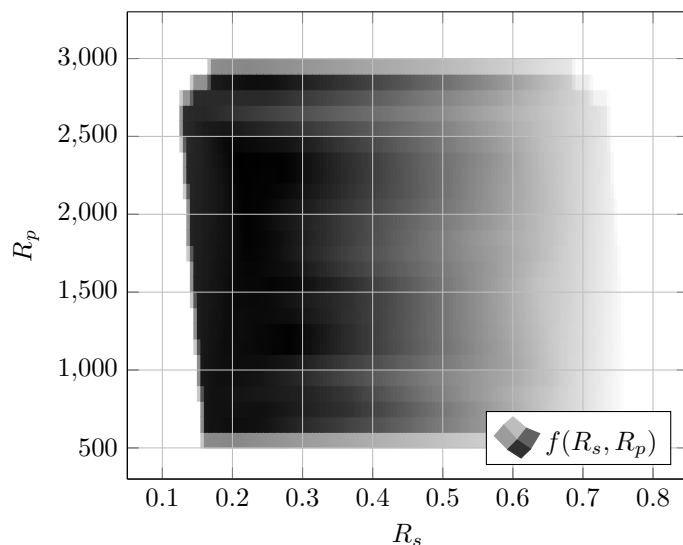


Figure 5. Variation of the resistor R_s as function of the resistor R_p .

Table III
PARAMETERS OF THE TEN BEST SOLUTIONS FOUND.

Solution	I_{ph}	I_{sat}	m	R_s	R_p
Solution 1	8.68	1.21e-08	1.196	0.206	2444.2
Solution 2	8.68	4.22e-10	1.027	0.286	500.5
Solution 3	8.68	6.49e-10	1.046	0.276	777.9
Solution 4	8.68	6.60e-09	1.162	0.221	1888.9
Solution 5	8.68	6.27e-10	1.046	0.282	1055.9
Solution 6	8.68	5.81e-10	1.041	0.286	1333.5
Solution 7	8.68	1.14e-09	1.072	0.275	2999.6
Solution 8	8.68	1.06e-09	1.067	0.275	2166.5
Solution 9	8.68	6.06e-10	1.043	0.287	1611.1
Solution 10	8.68	1.01e-09	1.065	0.277	2721.9

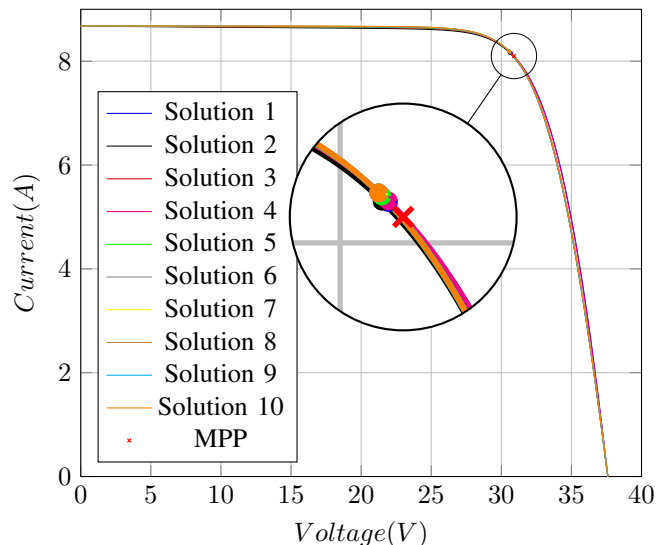


Figure 6. Characteristic curve of the pair voltage-current of the best 10 solutions found.

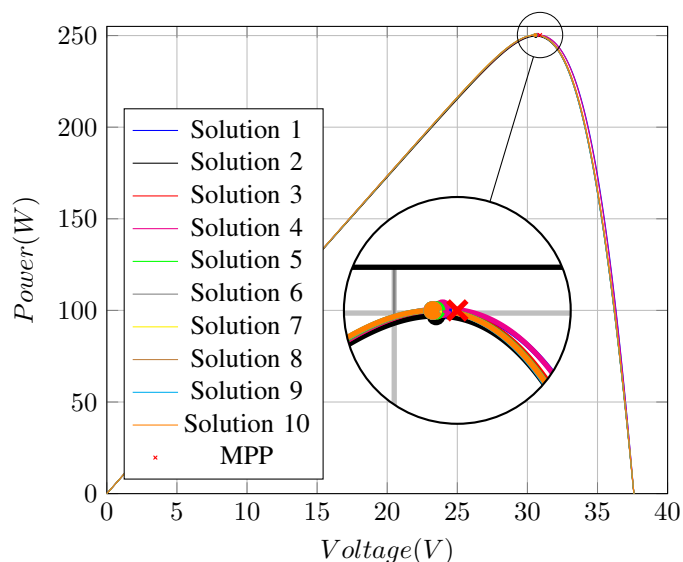


Figure 7. Characteristic curve of the pair voltage-power of the best 10 solutions found.

of view of accuracy, may not be a good practice since the value of the resistor R_p , for some values of R_s and of the diode ideality factor m cannot be consider infinite (this assumption constitutes a simplification for determining the parameters); (ii) once multiple optimum solutions are attained, the resolution of the equation system may not be a good option since it will converge to a solution close to the initial condition and this may not be the optimum solution; (iii) accordingly to what has been presented, the best option is clearly the employment of optimization methods, as the one used in the present work.

V. CONCLUSION

This paper has shown the capacity, the flexibility and the precision of the proposed method, as established in the discussion of the previous section, where it was reached the conclusion that the best option for determining the parameters that characterize the mathematical model is through optimization algorithms. Also, the method can be used for any existing model and performing both under the reference conditions and as out off these conditions. By the experiments held, the photovoltaic parameter extraction is a very hard multimodal problem, so that, the best option is clearly the employment of optimization methods, as the one used in the present work.

ACKNOWLEDGMENT

This work was supported by National Funding from the FCT-Fundação para a Ciência e a Tecnologia, through the UID/EEA/50008/2013 Project.

REFERENCES

- [1] A. N. Celik and N. Acikgoz, "Modelling and experimental verification of the operating current of mono-crystalline photovoltaic modules using four- and five-parameter models," *Applied Energy*, vol. 84, no. 1, pp. 1–15, jan 2007.
- [2] W. De Soto, S. Klein, and W. Beckman, "Improvement and validation of a model for photovoltaic array performance," *Solar Energy*, vol. 80, no. 1, pp. 78–88, jan 2006.
- [3] S. B. Dongue, "A new strategy for accurately predicting electrical characteristics of PV modules using a nonlinear five-point model," *Journal of Energy*, vol. 2013, no. 2, 2013.
- [4] A. Ortiz-Conde, D. Lugo-Muoz, and F. J. Garcia-Sanchez, "An explicit multiexponential model as an alternative to traditional solar cell models with series and shunt resistances," *IEEE Journal of Photovoltaics*, vol. 2, no. 3, pp. 261–268, July 2012.
- [5] W. D. Soto, "Improvement and validation of a model for photovoltaic array performance," Ph.D. dissertation, Solar Energy Laboratory University of Wisconsin-Madison, 2004.
- [6] M. Villalva, J. Gazoli, and E. Filho, "Comprehensive Approach to Modeling and Simulation of Photovoltaic Arrays," *IEEE Transactions on Power Electronics*, vol. 24, no. 5, pp. 1198–1208, may 2009.
- [7] D. Sera, R. Teodorescu, and P. Rodriguez, "PV panel model based on datasheet values," in *2007 IEEE International Symposium on Industrial Electronics*. IEEE, jun 2007, pp. 2392–2396.
- [8] E. Matagne, R. Chenni, and R. El Bachtiri, "A photovoltaic cell model based on nominal data only," in *2007 International Conference on Power Engineering, Energy and Electrical Drives*. IEEE, apr 2007, pp. 562–565.
- [9] F. Ghani and M. Duke, "Numerical determination of parasitic resistances of a solar cell using the Lambert W-function," *Solar Energy*, vol. 85, no. 9, pp. 2386–2394, sep 2011.
- [10] N. Femia, G. Petrone, G. Spagnuolo, and M. Vitelli, *Power Electronics and Control Techniques for Maximum Energy Harvesting in Photovoltaic Systems*, ser. Industrial Electronics. CRC Press, dec 2012, vol. 20125477.
- [11] V. Lo Brano, G. Ciulla, and M. Di Falco, "Artificial Neural Networks to Predict the Power Output of a PV Panel," *International Journal of Photoenergy*, vol. 2014, pp. 1–12, 2014.
- [12] M. Balzani and A. Reatti, "Neural network based model of a PV array for the optimum performance of PV system," in *Research in Microelectronics and Electronics, 2005 PhD*, vol. 2. IEEE, 2005, pp. 123–126.
- [13] M. Elhagry, A. Elkousy, M. Saleh, T. Elshatter, and E. Abou-Elzahab, "Fuzzy modeling of photovoltaic panel equivalent circuit," in *Proceedings of 40th Midwest Symposium on Circuits and Systems. Dedicated to the Memory of Professor Mac Van Valkenburg*, vol. 1. IEEE, 1997, pp. 60–63.
- [14] J. J. Soon and K.-S. Low, "Photovoltaic Model Identification Using Particle Swarm Optimization With Inverse Barrier Constraint," *IEEE Transactions on Power Electronics*, vol. 27, no. 9, pp. 3975–3983, sep 2012.
- [15] C. Saravanan, "A Comprehensive Analysis for Extracting Single Diode PV Model Parameters by Hybrid GA-PSO Algorithm," vol. 78, no. 8, pp. 78–81, 2013.
- [16] K.-S. Low, "Optimizing photovoltaic model parameters for simulation," in *2012 IEEE International Symposium on Industrial Electronics*. IEEE, may 2012, pp. 1813–1818.
- [17] G. Blaesser and E. Rossi, "EXTRAPOLATION OF OUTDOOR MEASUREMENTS OF PV ARRAY," vol. 25, pp. 91–96, 1988.
- [18] A. J. Anderson, "Photovoltaic Translation Equations: A New Approach," pp. 604–612, 1996.
- [19] B. Marion, "A method for modeling the current-voltage curve of a PV module for outdoor conditions," *Progress in Photovoltaics: Research and Applications*, vol. 10, no. 3, pp. 205–214, may 2002.
- [20] F. Ghani, G. Rosengarten, M. Duke, and J. Carson, "The numerical calculation of single-diode solar-cell modelling parameters," *Renewable Energy*, vol. 72, pp. 105–112, dec 2014.
- [21] K. Ishaque and Z. Salam, "An improved modeling method to determine the model parameters of photovoltaic (PV) modules using differential evolution (DE)," *Solar Energy*, vol. 85, no. 9, pp. 2349–2359, sep 2011.
- [22] B. Romero, G. del Pozo, and B. Arredondo, "Exact analytical solution of a two diode circuit model for organic solar cells showing S-shape using Lambert W-functions," *Solar Energy*, vol. 86, no. 10, pp. 3026–3029, oct 2012.
- [23] K. Ishaque, Z. Salam, and H. Taheri, "Simple, fast and accurate two-diode model for photovoltaic modules," *Solar Energy Materials and Solar Cells*, vol. 95, no. 2, pp. 586–594, feb 2011.
- [24] F. Ghani, M. Duke, and J. Carson, "Numerical calculation of series and shunt resistance of a photovoltaic cell using the Lambert W-function: Experimental evaluation," *Solar Energy*, vol. 87, pp. 246–253, jan 2013.
- [25] L. H. I. Lim, Z. Ye, J. Ye, D. Yang, and H. Du, "A linear identification of diode models from single $i-v$ characteristics of pv panels," *IEEE Transactions on Industrial Electronics*, vol. 62, no. 7, pp. 4181–4193, July 2015.
- [26] C. P. Lim, L. C. Jain, and S. Dehuri, Eds., *Innovations in Swarm Intelligence*, ser. Studies in Computational Intelligence. Berlin, Heidelberg: Springer Berlin Heidelberg, 2009, vol. 248.
- [27] X. S. Yang, *Studies in Computational Intelligence 516 Cuckoo Search and Firefly Algorithm*, 2013.
- [28] B. K. Panigrahi, Y. Shi, and M.-H. Lim, *Handbook of Swarm Intelligence: Concepts, Principles and Applications*, 2011, vol. 8.